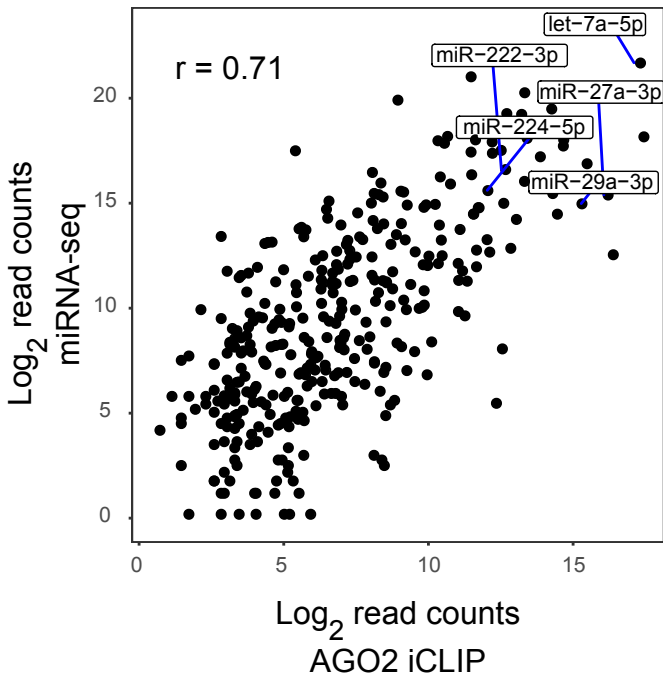
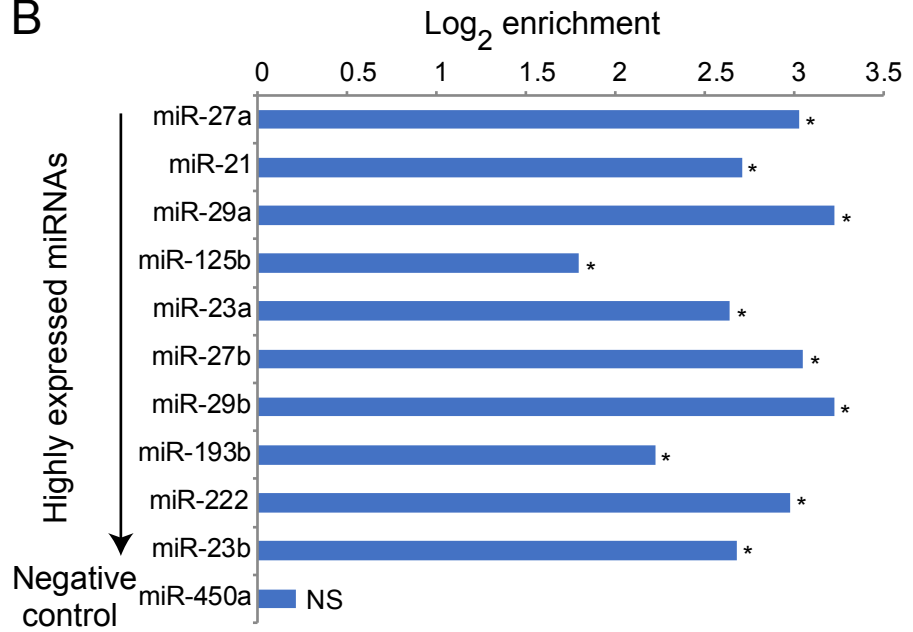


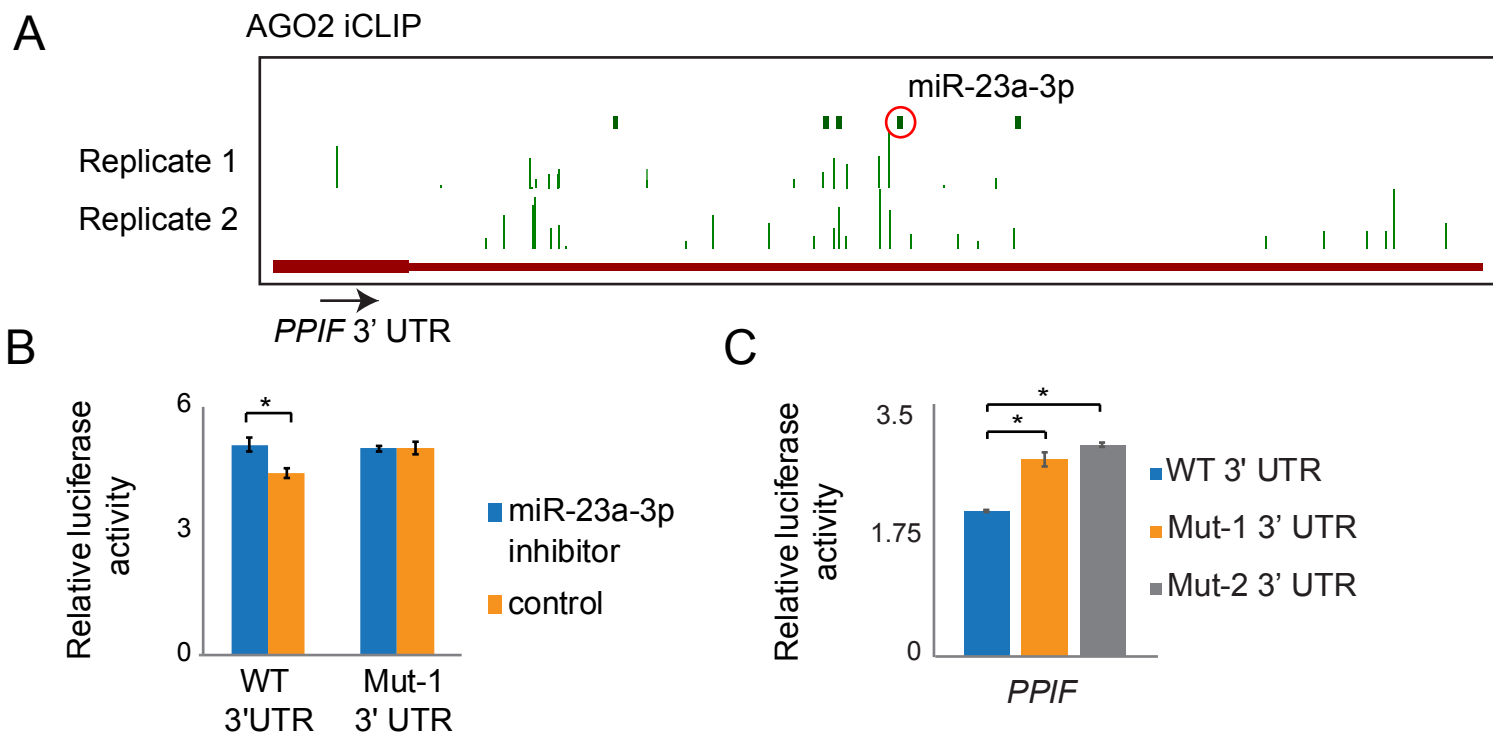
A



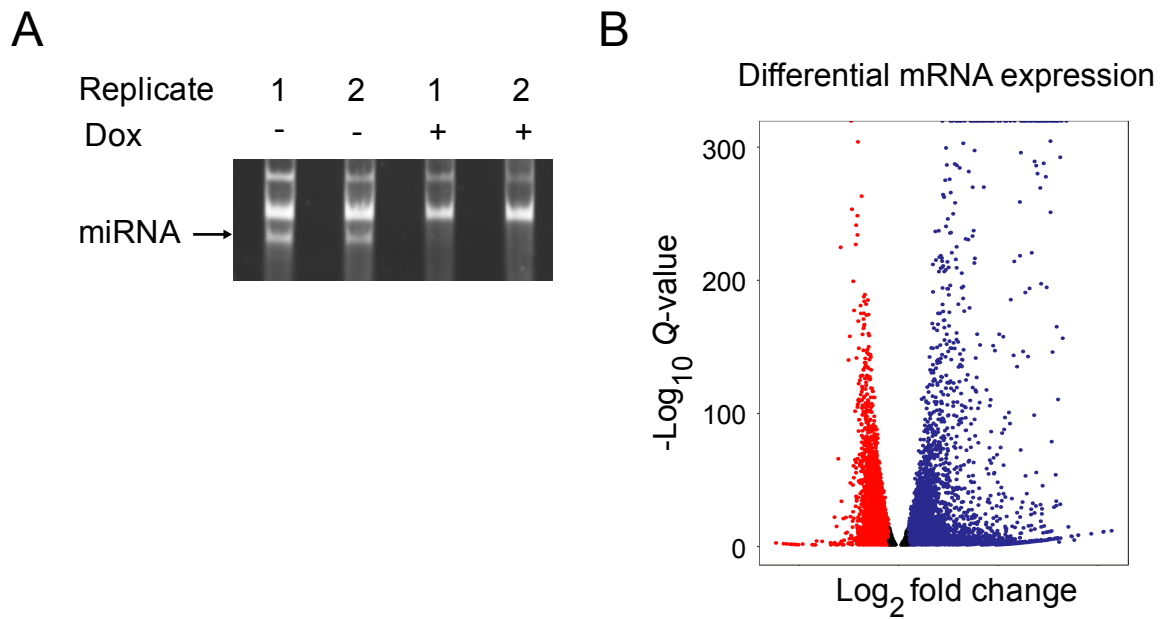
B



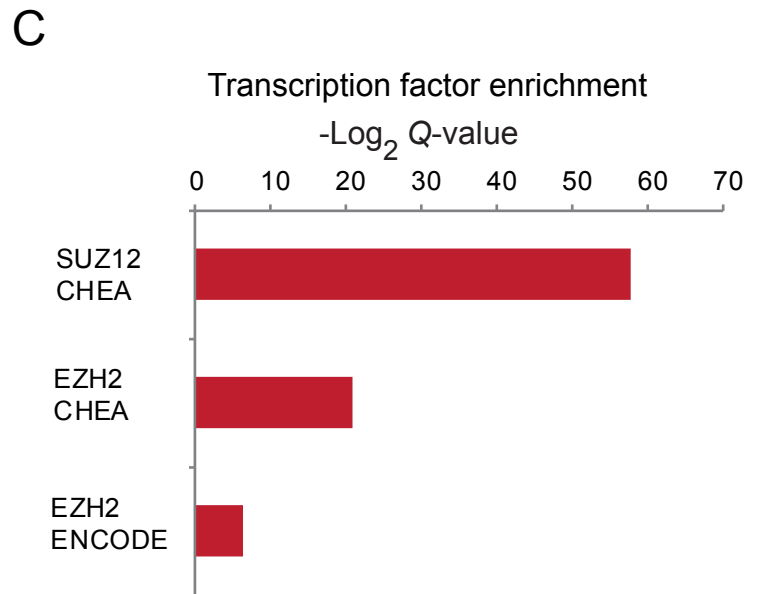
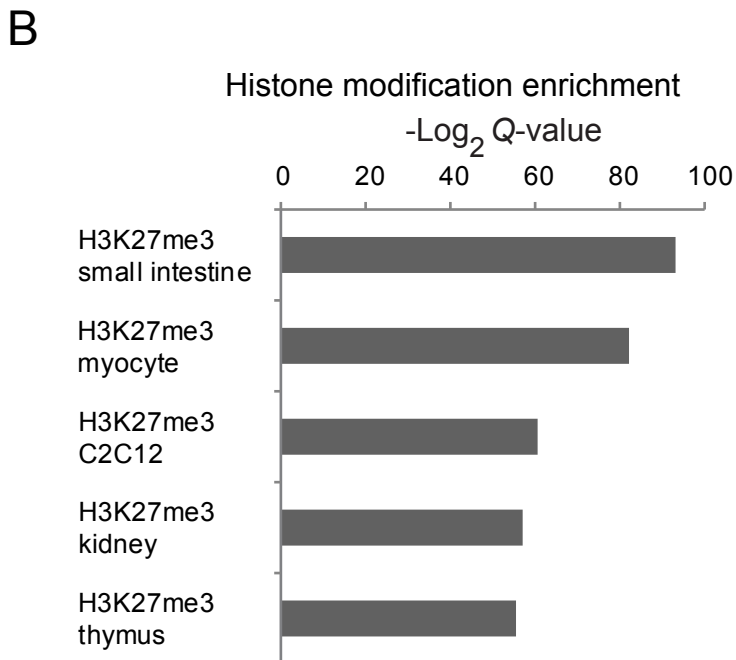
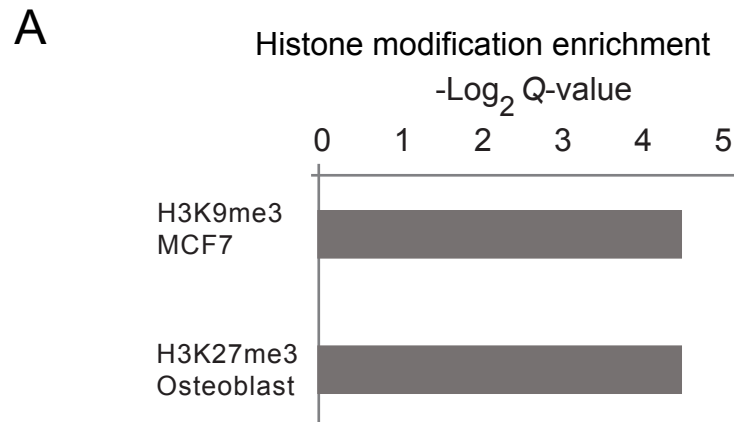
Supplemental Figure S1. AGO2 binding sites identified by iCLIP are enriched for binding sites of highly expressed miRNAs. (A) Correlation of miRNA enrichment in AGO2 iCLIP data (X-axis) with their expression (Y-axis). AGO2 iCLIP-enriched miRNAs shown in Fig 1D (right) are indicated. (B) Enrichment for predicted mRNA targets of AGO2-interacting miRNAs among protein-coding genes interacting with AGO2.



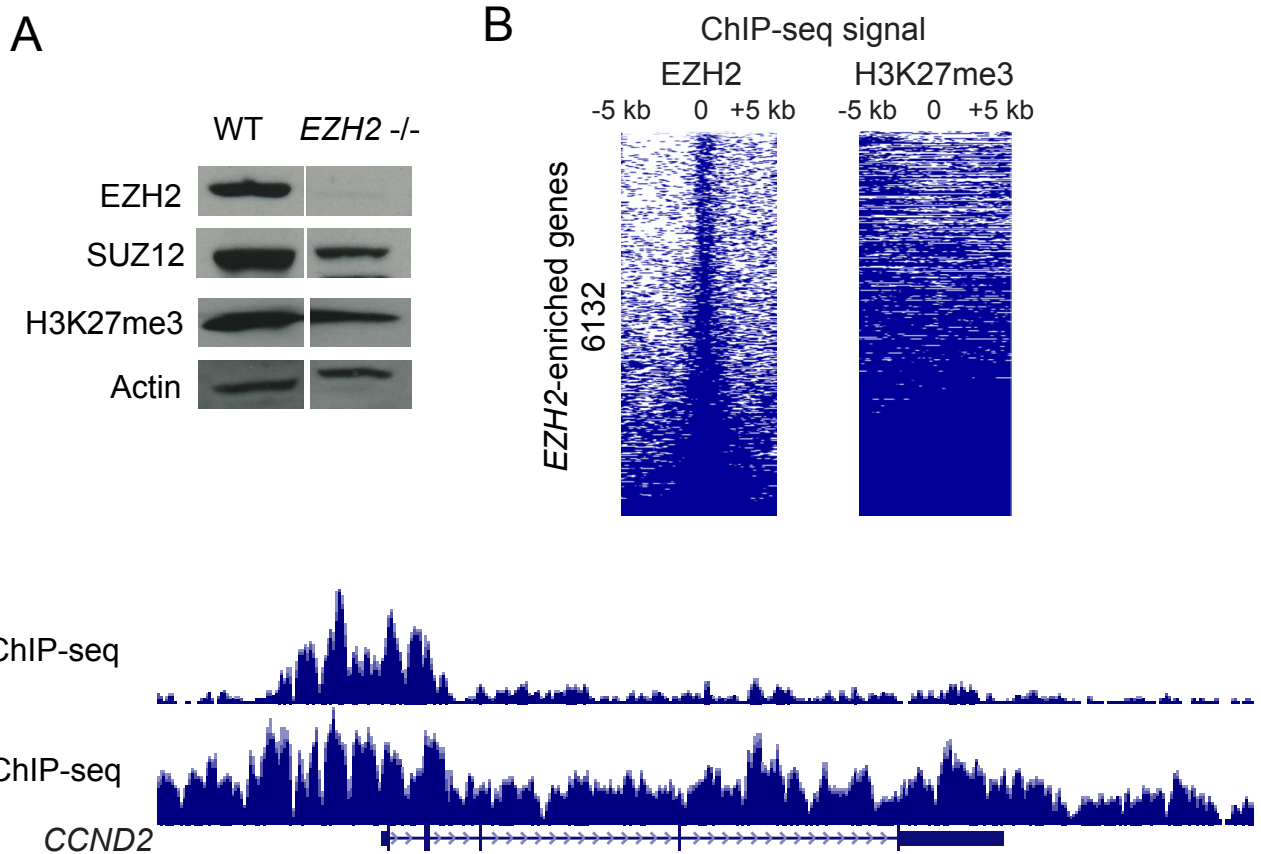
Supplemental Figure S2. miR-23a-3p directly represses *PPIF* expression. (A) Genome browser view showing AGO2 iCLIP peaks at the 3' UTR of *PPIF*. Green bars represent predicted miRNA binding sites with miR-23a-3p binding site highlighted in red. (B) Luciferase assays showing rescue of miRNA inhibition on treatment with miR-23a-3p inhibitor or negative control inhibitor for WT 3' UTR and mutant 3' UTR (seed deletion, Mut-1) transfected U87MG cells. (C) Changes in luciferase signal on deletion of miR-23a-3p binding site (Mut-1) or disruption of miRNA-*PPIF* interactions through base substitutions (Mut-2) in T98G cells.



Supplemental Figure S3. Identification of miRNA-repressed genes by global depletion of miRNAs. (A) cDNA libraries prepared from miRNA depleted (+ Dox) and non-depleted (- Dox) T98G cells. (B) Volcano plot of differentially expressed protein-coding genes in response to VP55 induction.

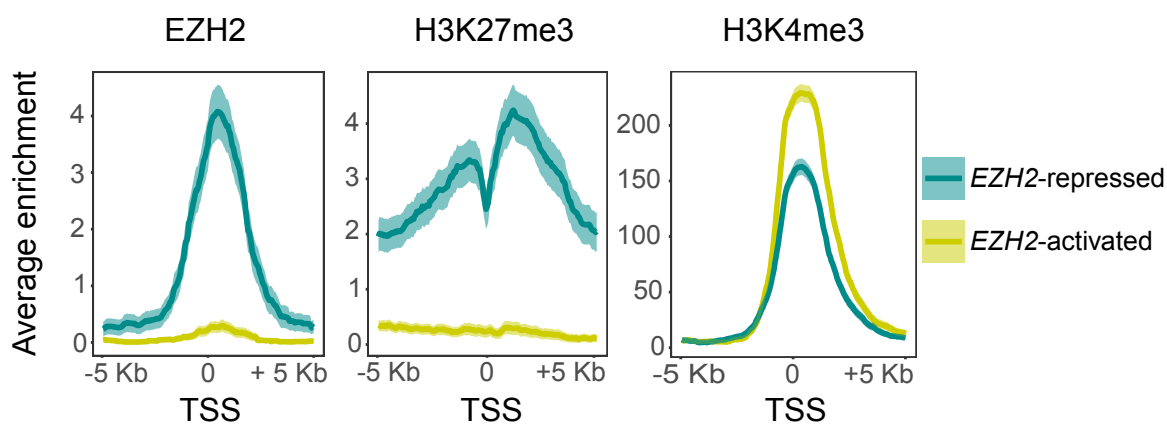


Supplemental Figure S4. Gene set enrichment analysis using Enrichr. (A) Enrichr analysis showing enrichment for histone modifications at a control set of genes expressed in the same range as the miRNA-repressed genes identified in T98G cells. (B,C) Enrichr analysis showing enrichment for H3K27me3 (B) and PRC2 (C) at genes up-regulated in miRNA-depleted mESCs (DICER knockout mESCs).

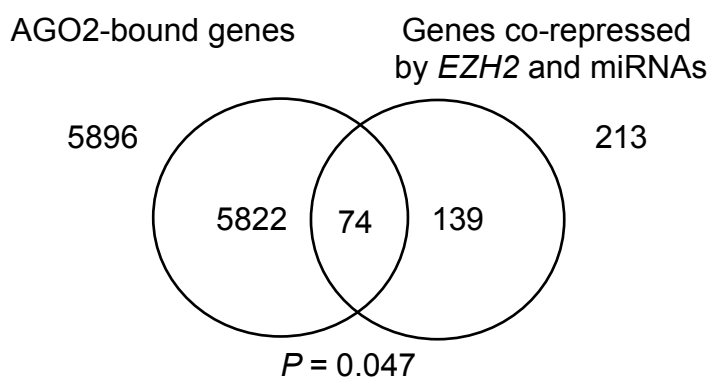


Supplemental Figure S5. (A) Immunoblots for EZH2, SUZ12 and H3K27me3 in WT and *EZH2*^{-/-} cells. (B) EZH2 and H3K27me3 ChIP-seq enrichment scores for protein-coding genes containing at least one significant EZH2 ChIP peak. Each row represents a gene containing at least one EZH2 ChIP-seq peak and the columns are binned into 50 bp windows spanning 10 kb around the TSS. (C) Genome browser view of *CCND2*, a gene enriched with EZH2 and H3K27me3 on chromatin, and that is derepressed in *EZH2*^{-/-} cells.

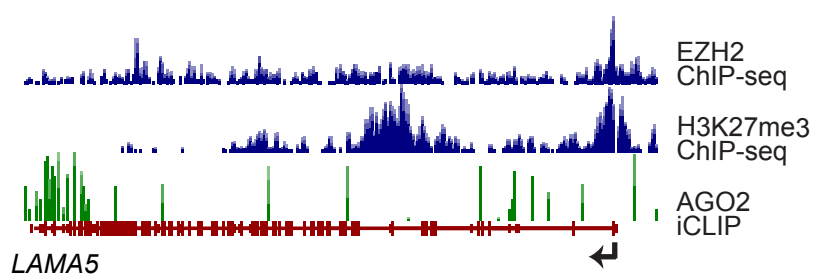
A



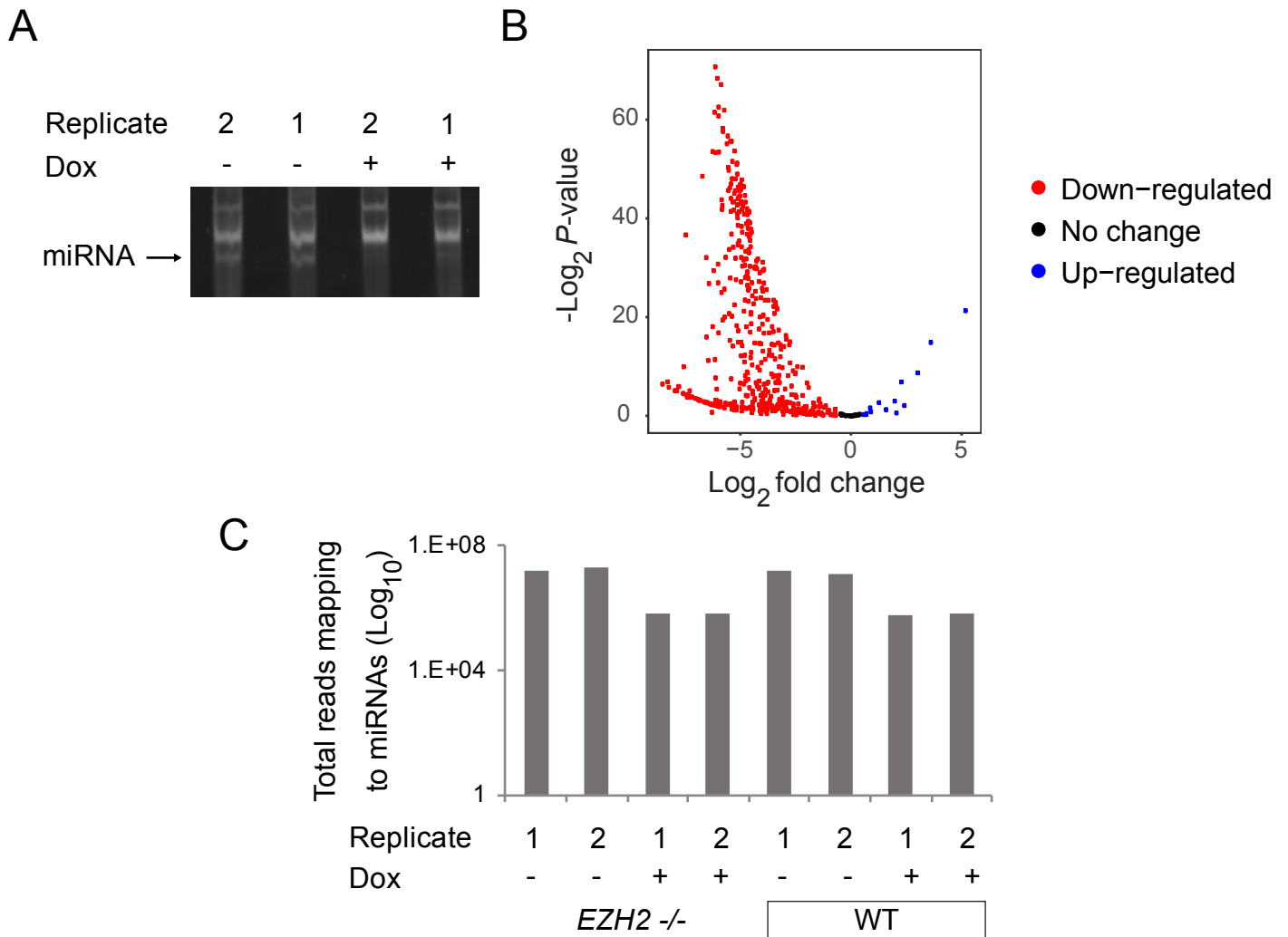
B



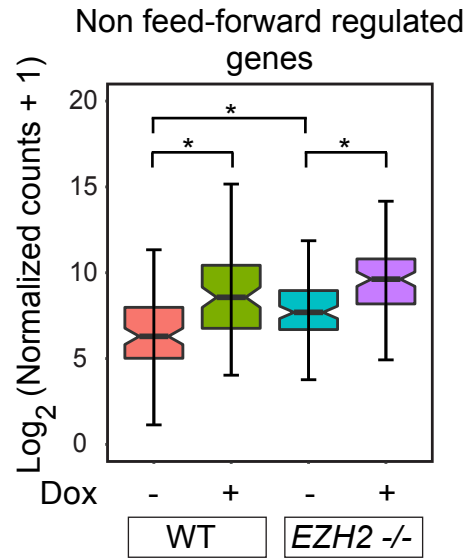
C



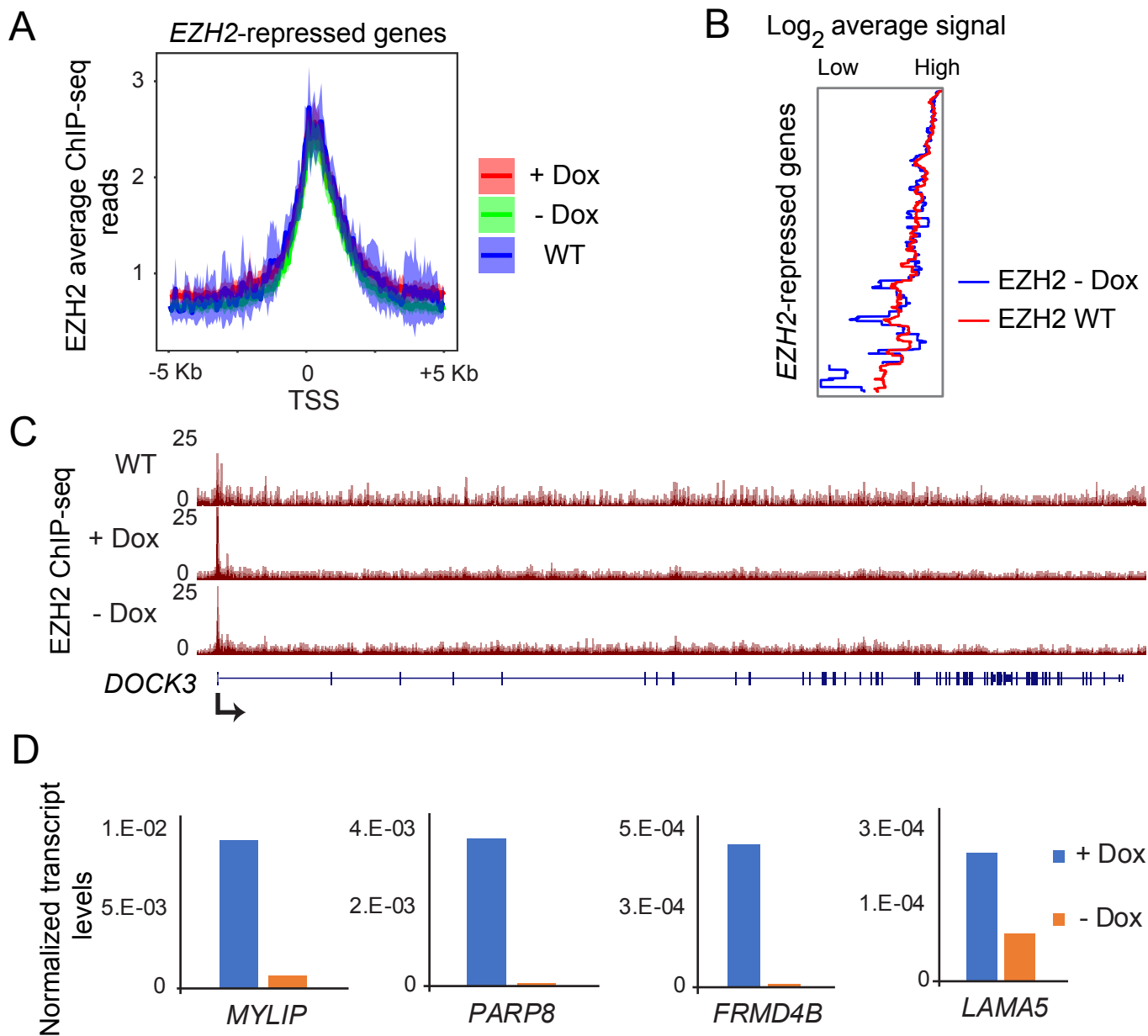
Supplemental Figure S6. Genes derepressed on loss of EZH2 are enriched for PRC2 and also regulated by miRNAs. (A) Normalized density of EZH2, H3K27me3 and H3K4me3 ChIP enrichment scores in the 10 kb region spanning the TSS of EZH2-regulated genes plotted in Fig. 3A. (B) Overlap of AGO2-interacting genes repressed by miRNAs and genes co-repressed by *EZH2* and miRNAs. Significance of overlap was calculated using the hypergeometric test. (C) Genome browser view of *LAMA5*, a gene enriched with EZH2 and H3K27me3 on chromatin, and whose transcript is also bound by AGO2.



Supplemental Figure S7. Global miRNA depletion in *EZH2* *-/-* cells is comparable to WT cells. (A) cDNA libraries prepared from *EZH2* *-/-* cells with (+ Dox) and without depletion of miRNAs (- Dox). (B) Volcano plot of differentially expressed miRNAs in response to *VP55* induction. X-axis represents \log_2 fold difference between expression of miRNAs in *VP55*-induced and non-induced cells. Y-axis represents $-\log_2$ P-value of the expression difference calculated using DESeq2. (C) Total miRNA counts (Log_{10} total reads mapping to miRNAs) in WT and *EZH2* *-/-* cells with and without depletion of miRNAs.

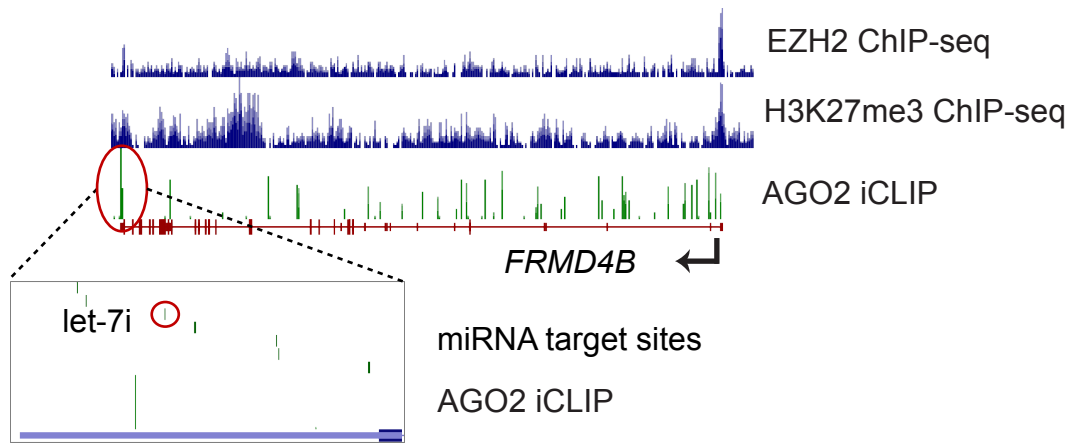


Supplemental Figure S8. Non feed-forward regulated genes show derepression in response to miRNA loss in *EZH2*^{-/-} cells and WT T98G cells. Box plot comparing expression of non-feed-forward regulated genes in miRNA depleted and non-depleted WT and *EZH2*^{-/-} cells.

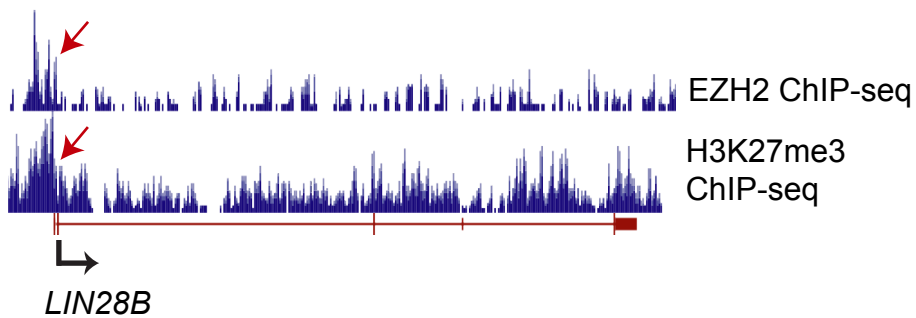


Supplemental Figure S9. EZH2 ChIP-seq in *VP55*-integrated WT - Dox cells is consistent with EZH2 ChIP-seq in WT cells. (A) Normalized density of EZH2 ChIP-seq reads at *EZH2*-repressed genes from EZH2 ChIP-seq in *VP55*-integrated WT + Dox, WT - Dox and WT cells. (B) Average EZH2 ChIP-seq signal for genes plotted in B. (C) Genome browser view of *DOCK3*, showing EZH2 enrichment in WT T98G cells, WT + Dox and WT - Dox cells. (D) qRT-PCR validation of Dox-induced derepression of miRNA-repressed genes, plotted as in Fig. 1E and normalized to Actin.

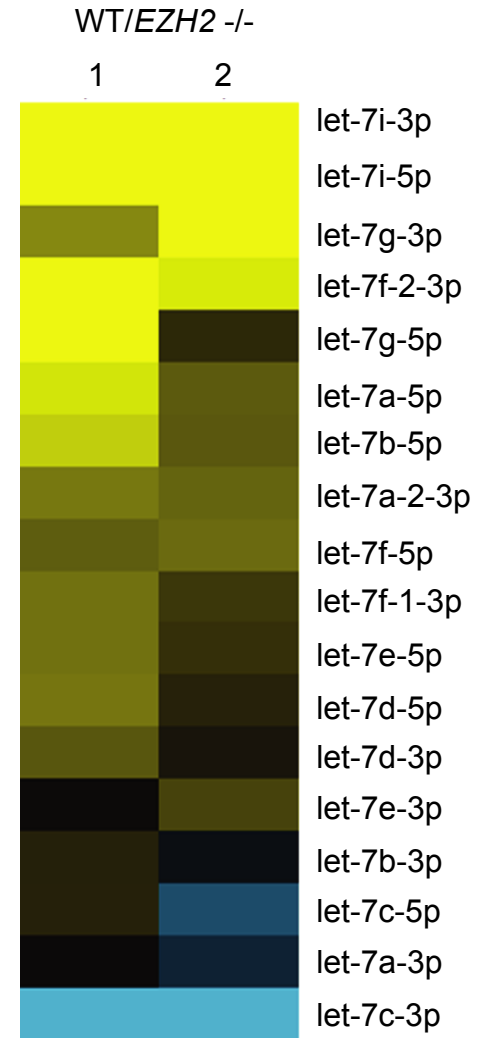
A



B

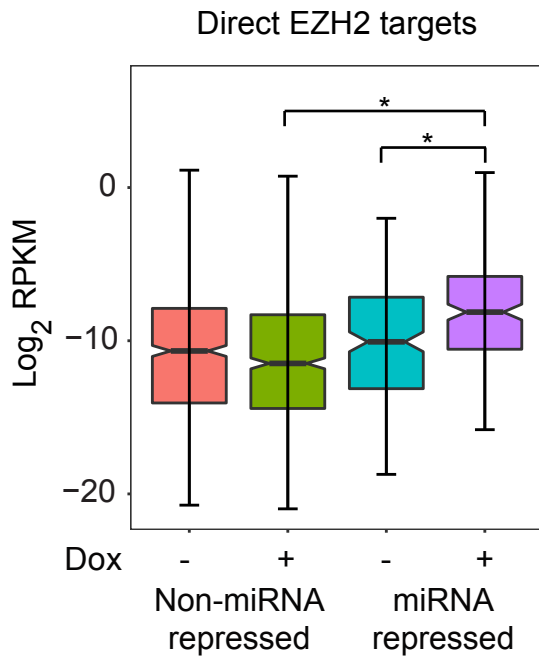


C

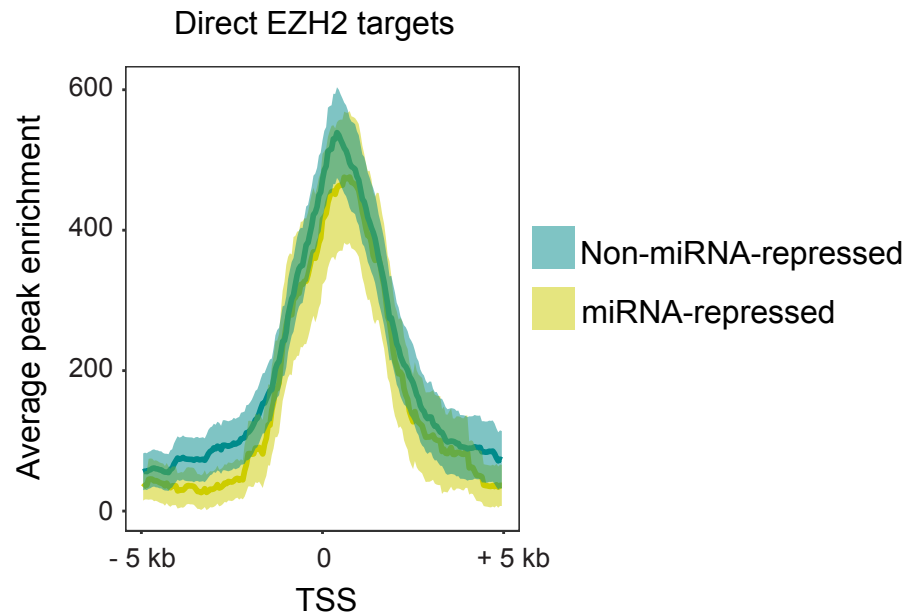


Supplemental Figure S10. *EZH2* activates let-7 miRNAs by directly repressing *LIN28B*. (A) Genome browser view of *FRMD4B* showing tracks for H3K27me3 ChIP-seq, *EZH2* ChIP-seq and AGO2 iCLIP highlighting the binding site for let-7i. (B) Genome browser view of *LIN28B* showing tracks for *EZH2* and H3K27me3 ChIP-seq. (C) Heatmap showing expression change of all let-7 miRNAs in WT and *EZH2* ^{-/-} cells. Rows are ranked by low to high log₂ fold change (WT/*EZH2* ^{-/-}).

A



B



Supplemental Figure S11. Genes co-repressed by *EZH2* and miRNAs are less tightly repressed by *EZH2* than genes silenced by *EZH2* alone. (A) Box plot showing average expression in Dox treated (miRNA depleted) and untreated WT cells for two sets of genes - PRC2-repressed genes that are not co-repressed by miRNAs (non-miRNA-repressed) and genes that are co-repressed by PRC2 and miRNAs (miRNA-repressed). (B) Normalized density of EZH2 ChIP enrichment scores in a 10 kb region spanning the TSS of PRC2 target genes that are either non-miRNA-repressed or miRNA-repressed.